A unified hydrophobicity scale for multispan membrane proteins

Julia Koehler,[1,3] Nils Woetzel,[1,3] René Staritzbichler,[1,3] Charles R. Sanders,[2,3] and Jens Meiler[1,3]*

[1] Department of Chemistry, Vanderbilt University, Nashville, Tennessee

[2] Department of Biochemistry, Vanderbilt University, Nashville, Tennessee

[3] Center for Structural Biology, Vanderbilt University, Nashville, Tennessee

ABSTRACT

The concept of hydrophobicity is critical to our understanding of the principles of membrane protein (MP) folding, structure, and function. In the last decades, several groups have derived hydrophobicity scales using both experimental and statistical methods that are optimized to mimic certain natural phenomena as closely as possible. The present work adds to this toolset the first knowledge-based scale that unifies the characteristics of both α-helical and β-barrel multispan MPs. This unified hydrophobicity scale (UHS) distinguishes between amino acid preference for solution, transition, and trans-membrane states. The scale represents average hydrophobicity values of amino acids in folded proteins, irrespective of their secondary structure type. We furthermore present the first knowledge-based hydrophobicity scale for mammalian α-helical MPs (mammalian hydrophobicity scale—MHS). Both scales are particularly useful for computational protein structure elucidation, for example as input for machine learning techniques, such as secondary structure or trans-membrane span prediction, or as reference energies for protein structure prediction or protein design. The knowledge-based UHS shows a striking similarity to a recent experimental hydrophobicity scale introduced by Hessa and coworkers (Hessa T et al., Nature 2007;450:U1026–U1032). Convergence of two very different approaches onto similar hydrophobicity values consolidates the major differences between experimental and knowledge-based scales observed in earlier studies. Moreover, the UHS scale represents an accurate absolute free energy measure for folded, multispan MPs—a feature that is absent from many existing scales. The utility of the UHS was demonstrated by analyzing a series of diverse MPs. It is further shown that the UHS outperforms nine established hydrophobicity scales in predicting trans-membrane spans along the protein sequence. The accuracy of the present hydrophobicity scale profits from the doubling of the number of integral MPs in the PDB over the past four years. The UHS paves the way for an increased accuracy in the prediction of trans-membrane spans.

INTRODUCTION

The hydrophobicity of an amino acid is related to its transfer free energy from a polar medium (such as the cytoplasm) to an apolar medium (like a membrane). Although the transfer free energy depends on the chemical nature of the two solvents, it also depends on the structural context of the amino acid residue. An obvious influence is the degree to which functional groups of an amino acid are exposed and hence available for interaction with the solvent. In turn, the transfer free energy of a single amino acid will be much different from the transfer free energy in a model peptide, which again will differ from the transfer free energy of an amino acid in the structural context of a folded protein, given the various levels of exposure to the solvent as well as the number of hydrogen bonds the residues participate in.

This picture of direct interactions between amino acid and solvent is further complicated because the transfer from one medium into another may trigger structural changes in model peptides or proteins that will affect the level of exposure of an amino acid.

Given the diverse biophysical properties of membranes in various compartments of the cell, the challenge

to model these complex systems accurately in experiments, and the different structural contexts in which amino acids are transferred from one medium into another make it impossible to design a single transfer free energy scale that is optimal under all circumstances. The existence of many transfer free energy scales is a logical consequence.

An older experimental scale is that of Hopp and Woods (HW),[1] who described a hydrophilicity scale to predict antigenic sites on proteins. Goldman, Engelman, and Steitz (GES) derived a hydrophobicity scale based on energetic considerations of residues in α-helices.[2] Wimley and White (WW) achieved a significant step forward[3–6] by introducing a three-state scale based on experimental hydrophobicities between water interface and water bilayer in model systems.

Although most hydrophobicity scales have been derived experimentally, there are also examples of knowledge-based approaches: A database of known protein structures is utilized to derive free energies from statistics using an inverse Boltzmann relation. Advantages of knowledge-based hydrophobicity scales include flexibility in the choice of the composition of the database—e.g., all folded, multi-span membrane proteins (MPs). In turn, the reference point of the scale as well as the absolute size of the hydrophobicity values will match the chosen dataset and accurately describe the characteristics of amino acids in multi-span MPs. In contrast, an experimental scale (e.g., derived for α-helical peptides) will display a bias in absolute size of the hydrophobicity values as well as the reference point when used in the context of folded, multispan MPs.

One of the oldest knowledge-based scales was published by Janin[7] who used the known X-ray structures of 22 soluble proteins and derived a scale based on burial versus solvent accessibility of residues. In 2003 Punta and Maritan (PM)[8] derived knowledge-based hydrophobicity scales from two databases containing 118 and 228 trans-membrane α-helices, respectively. Very recently, Senes et al. derived a knowledge-based potential where the energy is dependent on the depth of the residue in the membrane bilayer.[9]

It has been common in the past to derive consensus hydrophobicity scales that seek to combine the advantages of several approaches. The scale by Kyte and Doolittle (KD)[10] is based on a variety of experimental observations from the literature[11–14] and uses the display method of Rose et al.[15,16] to detect trans-membrane spans along the protein sequence. Eisenberg et al. (EW)[17] published a consensus hydrophobicity scale derived from five different scales. In 1985, Guy[18] developed a scale based on statistical and experimental results of several studies.[7,11,12,19–22]

For most of the experimentally derived scales, the range of hydrophobicity values is rather large in comparison to the knowledge-based ones (Fig. 1). This is expected because experimentally derived scales use mostly model peptides that form α-helices where the residue in
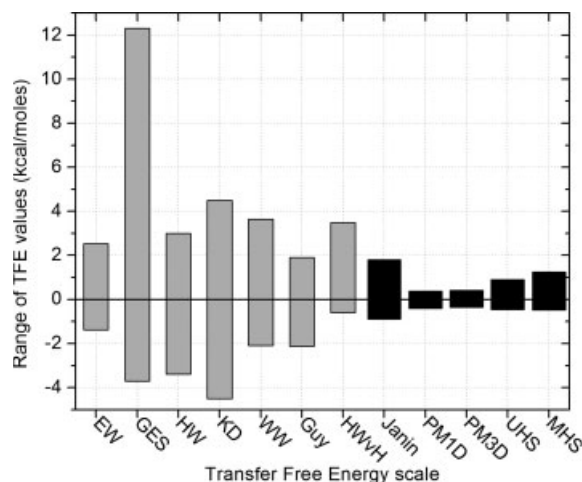

Figure 1

The diagram shows the range of transfer free energy values in kcal/moles for the different scales (EW: Eisenberg and Weiss; GES: Goldman, Engelman, Steitz; HW: Hopp and Woods; KD: Kyte and Doolittle; WW: Wimley and White; HWvH: Hessa, White and von Heijne; PM: Punta and Maritan; UHS: Unified Hydrophobicity Scale derived here; MHS: Mammalian Hydrophobicity Scale derived here). Note that the last five scales are knowledge-based scales and cover a much smaller range of values than any of the other scales.

question is exposed and other structural context is removed. These scales capture neatly the nature of the chemical interactions between apolar solvent and amino acid side chains. In contrast, knowledge-based scales derive statistics from multispan MPs to arrive at a hydrophobicity that might be biologically more relevant in the structural context of intact proteins. In multispan MPs, polar residues are somewhat more likely to occur in the membrane because these side chains can be buried from the interaction with the apolar membrane.

To this end, a remarkable series of experiments has been carried out by Hessa et al. in the von Heijne laboratory[23,24] leading to a "biological" hydrophobicity scale for α-helical proteins. By measuring the ratio of singly vs. doubly glycosylated Lep molecules that insert into the membrane bilayer via the Sec61 translocon, a "biological" hydrophobicity scale[24] was derived. This study has been beautifully extended[23] to a position-dependent free energy scale across a 19-residue α-helix that inserts into the membrane. These experimentally derived "biological" hydrophobicities match our knowledge-based ones very closely (see below).

Obviously, highly specialized hydrophobicity scales can be derived if assumptions regarding secondary structure (such as separation of α-helices from β-strands) or tertiary structure (such as level of exposure) are made. For instance, Beuming and Weinstein derived a knowledge-based prediction method to distinguish between the burial and exposure of certain amino acids.[25,26] Another example is the ROSETTAMEMBRANE algorithm, which

features a knowledge-based potential for folding of α-helical MPs.[27–29]

The objective of this work, however, is to derive a hydrophobicity scale for multispan integral MPs with no *a priori* assumptions regarding secondary or tertiary structure (structural context). This scale measures the likelihood of an amino acid to reside in membrane, transition, or soluble region within a folded protein. The scale can be used as absolute reference energy for folded multispan MPs, applied in protein structure elucidation, for example as input for machine learning techniques for the prediction of secondary structure, trans-membrane spans, or other structural features, or as reference energy for MP folding simulations or design. The scale is optimized to describe the characteristics of both α-helical proteins and β-barrels equally well. One application of the scale is the prediction of trans-membrane spans from amino acid sequence only, a method that could be applied to detect integral MPs in ORFs of newly sequenced genomes where no structural information is available, or in the early stages of a MP structure determination project. In addition, the identification of a MP or membrane spanning regions within a sequence is of particular interest in the initial phase of *de novo* computational tertiary structure prediction of proteins.[27] Furthermore, we derived a specialized hydrophobicity scale from α-helical mammalian MPs only to be able to identify α-helical trans-membrane spans in the human genome and the genome of other mammals.

To demonstrate the usefulness of these scales for such applications and to allow comparison with other hydrophobicity scales, we implemented a simple version of a prediction scheme for trans-membrane regions: The hydrophobicity values are averaged over a window of 15 residues. Although we realize that this simple scheme is sub-optimal to achieve high-quality predictions in particular for β-barrel proteins, it proves efficient to benchmark these scales and compare them to other hydrophobicity scales.

METHODS

Creation of the databases of nonredundant multispan membrane proteins

Knowledge-based potentials are derived from a database of known properties and have shown to be especially suitable to describe features of proteins in structural biology.[30,31] For the derivation of such potentials, the ProteinDataBank (PDB) is an invaluable resource. It contains ~46,000 three-dimensional structures of soluble proteins and ~850 structures of MPs (as of 02/2008), about 70% of which are multispan MPs. Tusnady *et al.* compiled the PDBTM,[32] a sub-database of the PDB which contains all MPs and includes additional information such as the bilayer thickness for each protein deter-

mined by the TMDET algorithm.[33,34] In this database, coordinates of symmetric domains were reconstructed from the crystallographic symmetry transformations (SYMTR) in the PDB entry and conversely coordinates of redundant atoms (from crystallization) are removed. Furthermore, the protein is conveniently transformed into membrane coordinates with the z-axis representing the membrane normal.

For the derivation of the unified hydrophobicity scale (UHS), the complete list of multispan MPs from the PDBTM was submitted to the PISCES server[35,36] to identify proteins with low sequence similarity. The input parameters used for culling are the following: sequence percentage identity $\leq$ 25%, resolution $\leq$ 3.0 Å, R-factor $\leq$ 0.3, sequence length 40–10,000 amino acids. The resulting database of unique structures contained 60 MPs. Before proceeding with the analysis, all nonstandard amino acids were converted into the closest standard amino acid type. Further details about the composition of this database are given in the results section. For a complete list of all proteins see Supporting Table I.

For deriving the mammalian hydrophobicity scale (MHS), all MPs in the PDBTM were classified according to their host organism. The list of mammalian proteins (156 PDB entries in total) was culled with the PISCES server using the following culling parameters: sequence identity $\leq$ 25%, resolution $\leq$ 3.0 Å, R-factor $\leq$ 0.3, sequence length 40–10,000 amino acids. The resulting database consisted of 16 α-helical proteins (from cattle, human, mouse, pig, rat, rabbit, and sheep) with 12,389 residues in total. The PDB codes of these proteins are: 1afo, 1okc, 1p49, 1ppj, 1u19, 1v54, 1vry, 1wpg, 1zll, 1zoy, 2b6o, 2hac, 2hfe, 2jwa, 2uui, 2z9a. Because these proteins have large extra-membrane domains, only 2,563 residues were located in the membrane bilayer and the remaining 9,826 belonged to the soluble phase. For the three-state scenario, 2,563 residues were located in the TM, 3,122 in the TR, and 6,704 in the SOL. These biases were corrected by appropriate normalization procedures (see below).

Definition of membrane, transition, and soluble regions

We distinguish between two different scenarios: (a) the two-state scenario, where only the trans-membrane (TM) and soluble region (SOL) is defined and no transition region exists and (b) the three-state scenario, where trans-membrane, transition (TR), and soluble region exist. A UHS was derived for both scenarios. Although the two-state scenario allows for comparison with most of the published hydrophobicity scales, the three-state scenario gives a more comprehensive and detailed picture of free energies and can be compared with the Wimley and White hydrophobicity scale.[5]
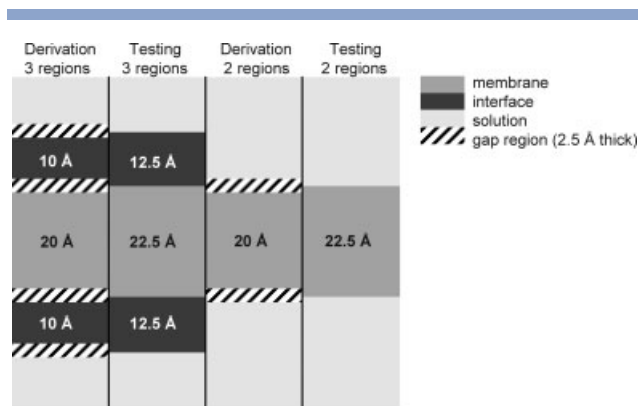
Figure 2

Definition of the different regions for the derivation and the testing of the scale in the two-state and three-state scenario. The gap region of 2.5 Å thickness was introduced to more cleanly distinguish between the different regions when deriving the scales. For the calculation of the agreements the prediction on a per-residue basis was compared to the "actual" locations of the regions (see testing in the figure). In the two-state scenario, the interface region was added to the SOL because its characteristics are more similar to the soluble phase than to the membrane interior.

In the three-state scenario, we assume a thickness of 20 Å for the TM core region.[37] On either side, this region is flanked by a 2.5 Å buffer zone, before the TR regions begins. Its thickness is assumed with 10 Å on either side of the membrane and connects to another buffer zone of 2.5 Å. Adjacent to this second buffer zone the SOL regions starts (Fig. 2).

In the two-state scenario, the SOL and TR regions are combined and the buffer zone between them vanishes. This procedure was chosen because SOL and TR share a higher similarity when compared to the TM region due to the polar headgroups of the lipid molecules.

The buffer zones were added to distinguish more cleanly between the different regions and account for differences in the membrane thicknesses when deriving the scales. We abstained from using the membrane layer thicknesses given in the PDBTM to avoid a somewhat recurrent influence of another prediction method on our results. We also found that usage of individual membrane thicknesses influenced the hydrophobicity values only marginally.

Derivation of amino acid propensities in the respective regions

To derive the free energies from the database the occurrence of each amino acid in each region was counted, which resulted in a total of 60 frequencies for the three-state scenario (20 amino acids × 3 regions) and 40 frequencies for the two-state scenario (20 amino acids × 2 regions). To eliminate a bias in the original

data with respect to any region, the number of amino acids in each region was normalized to 20. Afterwards, the propensity as defined by Shortle[38] was computed:

$$P = \frac{\text{number(region, AA)}/\text{number(region)}}{\text{number(AA)}/\text{number(total)}}. \quad (1)$$

The expected propensity for a randomly selected cell in the resulting matrix is 1, which is important for the proper definition of the reference energy (see below).

Translation of propensities into free energies

The resulting propensities P were used to derive the free energies, ΔG, for each amino acid in kcal/mol using the equation

$$\Delta G = -RT \ln P \quad (2)$$

with $R = k_B N_A$ (k_B being Boltzmann's constant and N_A being Avogadro's constant) at a temperature of $T = 293$ K. In the two-state scenario, one can rewrite Eq. (2) to directly derive the water to trans-membrane phase transfer free energies $\Delta\Delta G$ for each amino acid using the equation

$$\Delta\Delta G_{\text{TM}-\text{SOL}} = \Delta G_{\text{TM}} - \Delta G_{\text{SOL}} = -RT \ln\left(\frac{P_{\text{TM}}}{P_{\text{SOL}}}\right) \quad (3)$$

A corresponding equation applies for water to transition phase transfer.

Averaging of free energies over a sequence window of variable size for prediction

To obtain a prediction for a particular amino acid to be in one of the three regions (TM, TR, or SOL), the hydrophobicity values are averaged over a window of residues. Two different approaches for averaging were tested: (a) all residues within the window have the same weight (rectangular weight function), and (b) the central residue has the highest weight with a linear decrease towards the edges of the window where the weight is set to zero (triangular weight function). The resulting averaged free energy was utilized to predict the state of the central residue. Predictions over a complete sequence were achieved by sliding the window over the whole sequence (Supp. Fig. 2). Window sizes from one residue to 31 residues were tested. Only odd window sizes were considered to unambiguously assign a central residue.

Comparison of the hydrophobicity scales

To test the performance of the scale, the average value of the free energies over a certain window size was calcu-

lated for SOL, TR, and TM free energies in the three-state scenario, and TM and SOL region in the two-state scenario. The amino acid in the center of the window was assigned the state that corresponds to the lowest of the average energies. Agreement for a specific region was computed as percentage of correctly predicted amino acids. The overall agreement was computed by averaging the agreements in all regions. For the assignment of the correct state, the 2.5 Å buffer zones were split in half, that is, the TM region was 22.5 Å and the TR region was 12.5 Å thick with no buffer zones in between (Fig. 2).

Construction of datasets for cross-validation

To perform cross-validation and to obtain standard deviations for the free energies and transfer free energies, the database was divided into subsets. For the UHS, the dataset was divided into five subsets, where four sets were taken for the derivation and the performance was tested on the fifth independent set. All experiments were repeated five times with the independent test-set permuting through the five datasets. The subsets were chosen to contain approximately the same number of α-helix, β-strand, and coil residues (Supp. Table I). Because the proteins vary considerably in size, the numbers of proteins within the subsets fluctuate. A two-fold cross-validation was set up for the MHS as the dataset was significantly smaller with only 16 proteins.

Testing of the scale on four proteins

To test the algorithm four different example proteins from the PDBTM, which were not present in the MP-database of 60 proteins, were investigated. The examples comprise the voltage-gated potassium channel KcsA (PDB code 1K4C), the chloride channel ClC (PDB code 1KPK), the Glycerol facilitator protein GlfP (PDB code 1LDI), and the outer membrane protein W OmpW (PDB code 2FIT). The examples were chosen so as to test both α-helical and β-barrel proteins. Furthermore, the α-helical proteins present difficult examples because of short or broken α-helices as in GlfP and in the selectivity filter of KcsA and the unusually large tilt angles of the α-helices in ClC.

RESULTS AND DISCUSSION

Composition of the database of 60 nonredundant multispan membrane proteins

The database of 60 nonredundant multispan MPs encompasses a total of 43,523 amino acids, 31.4% of which reside in the TM region, 33.6% reside in the TR region, and 35.0% reside in the SOL region. Including the extra-membrane domains, 21 proteins were purely α-helical, five were purely β-strand, and 34 were mixed α-helical/β-strand proteins. Around 50% of all secondary structure elements reside in extra-membrane domains. In total, 977 α-helices (605 of which were TM) and 1056 β-strands (405 of which were TM) were present in the database. For a summary of these data see Supporting Table I. When deriving the free energy scales, amino acid counts were normalized by region to avoid a bias in the hydrophobicity values that resulted from an imbalanced database.

The two-state UHS allows direct comparison with other hydrophobicity scales

Most of the hydrophobicity scales in the literature have been derived for two regions, that is, no TR is defined [see Eq. (2)]. Although we strongly encourage ultimate usage of a three-state scale, a two-state UHS was derived in order to facilitate comparison with other methods. All hydrophobicity values are summarized in Table I and the characteristics of the different scales are given in Table II. Correlation with other hydrophobicity scales is plotted in Figure 3 and Supporting Figure 1.

Three-state UHS demonstrates the preference of Trp for interface region

Table III shows the free energy values in kcal/mol for all 20 amino acids and for all three regions (TM, TR, SOL). As for the two-state scenario, Cys has a large standard deviation for TM (0.09) and SOL (0.06) and its large value within TR indicates that it does not prefer to be in the TR. Ser and Thr have almost no preference for any of the three regions (Ser: TM = 0.02, TR = 0.02, SOL = −0.04; Thr: TM = −0.01, TR = 0.02, SOL = 0.00), which agrees with the findings of Senes[9] and Hessa.[23] The fact that Trp is often found in the TR[9,39–41] is confirmed by our results. It has been previously noted that Tyr also has a preference for the interface between TM and TR region. However, this preference of Tyr for the interface region is less distinct when compared with Trp.[9,23] In the UHS, Tyr shows a slight preference for residing within the TM region which could be a result of a slightly larger membrane thickness in our definition when compared with other scales.[23] Further, we find strong preferences for Ile, Phe, Leu, Val, and Met to be in the TM region and for Glu, Lys, Cys, Asp, and Gln to be in the SOL region.

The absence of structural context leads to less distinct free energy values relevant for multispan membrane proteins

It can be seen from Table I and Figure 1 that the values of knowledge-based hydrophobicity scales are in gen-

Table I
Values of the Water-Membrane Transfer Free Energies in kcal/mol

		Two-state scales														Three-state scales		
		Experimental				Consensus			Knowledge-based										
		HW[a]	GES[a]	WW	HWvH	EW[a]	KD[a]	Guy	Janin	PM$_{1D}$	PM$_{3D}$	UHS	SD	MHS	SD	WW$_{int}$	UHS$_{int}$	SD
Polar	C	−1.00	−2.00	−0.02	−0.13	−0.29	−2.50	−1.42	−0.90	−0.06	−0.15	0.01	0.15	0.01	0.02	−0.24	0.78	0.07
	N	0.20	4.80	0.85	2.05	0.78	3.50	0.48	0.50	0.18	0.22	0.50	0.03	0.55	0.03	0.42	−0.04	0.01
	Q	0.20	4.10	0.77	2.36	0.85	3.50	0.95	0.70	0.26	0.03	0.46	0.07	0.78	0.07	0.58	0.18	0.04
	S	0.30	−0.60	0.46	0.84	0.18	0.80	0.52	0.10	0.05	0.16	0.06	0.04	0.18	0.39	0.13	0.06	0.04
	T	−0.40	−1.20	0.25	0.52	0.05	0.70	0.07	0.20	0.02	−0.08	−0.01	0.01	−0.05	0.01	0.14	0.02	0.01
Charged	D	3.00	9.20	3.64	3.49	0.90	3.50	0.78	0.60	0.37	0.41	0.73	0.05	1.10	0.26	1.23	0.13	0.04
	E	3.00	8.20	3.63	2.68	0.74	3.50	0.83	0.70	0.15	0.30	0.70	0.03	1.09	0.08	2.02	0.41	0.02
	K	3.00	8.80	2.80	2.71	1.50	3.90	1.40	1.80	0.32	0.24	0.90	0.04	1.24	0.15	0.99	0.09	0.04
	R	3.00	12.30	1.81	2.58	2.53	4.50	1.91	1.40	0.37	0.32	0.55	0.05	1.24	0.17	0.81	0.04	0.02
Apolar	A	−0.50	−1.60	0.50	0.11	−0.62	−1.80	0.10	−0.30	−0.17	−0.15	−0.16	0.03	−0.24	0.01	0.17	0.02	0.02
	G	0.00	−1.00	1.15	0.74	−0.48	0.40	0.33	−0.30	0.01	0.08	−0.20	0.03	−0.10	0.06	0.01	−0.25	0.02
	I	−1.80	−3.10	−1.12	−0.60	−1.38	−4.50	−1.13	−0.70	−0.28	−0.29	−0.39	0.03	−0.43	0.01	−0.31	−0.06	0.03
	L	−1.80	−2.80	−1.25	−0.55	−1.06	−3.80	−1.18	−0.50	−0.28	−0.36	−0.30	0.03	−0.48	0.07	−0.56	−0.08	0.03
	M	−1.30	−3.40	−0.67	−0.10	−0.64	−1.90	−1.59	−0.40	−0.26	−0.19	−0.20	0.02	−0.17	0.09	−0.23	−0.12	0.06
	P	0.00	0.20	0.14	2.23	−0.12	1.60	0.73	0.30	0.13	0.15	0.50	0.04	0.50	0.11	0.45	0.07	0.03
	V	−1.50	−2.60	−0.46	−0.31	−1.08	−4.20	−1.27	−0.60	−0.17	−0.24	−0.25	0.02	−0.35	0.04	0.07	0.09	0.02
Aromatic	F	−2.50	−3.70	−1.71	−0.32	−1.19	−2.80	−2.12	−0.50	−0.41	−0.22	−0.46	0.04	−0.43	0.10	−1.13	−0.36	0.02
	H	−0.50	3.00	2.33	2.06	0.40	3.20	−0.50	0.10	−0.02	0.06	0.38	0.05	0.64	0.47	0.96	−0.07	0.05
	W	−3.40	−1.90	−2.09	0.30	−0.81	0.90	−0.51	−0.30	−0.15	−0.28	−0.03	0.03	−0.06	0.01	−1.85	−0.38	0.04
	Y	−2.30	0.70	−0.71	0.68	−0.26	1.30	−0.21	0.40	−0.09	−0.03	−0.12	0.04	0.23	0.17	−0.94	0.01	0.02

HW, Hopp and Woods[1]; GES, Goldman, Engelman, Steitz[2]; WW, Wimley and White[5]; HWvH, Hessa, White, and von Heijne[24]; EW, Eisenberg and Weiss[17]; KD, Kyte and Doolittle[10]; Guy, Guy[18]; Janin, Janin[7]; PM1D and PM3D, Punta and Maritan[8]; UHS, the knowledge-based scale derived in this article with its standard deviation (SD); MHS, the mammalian scale derived here with its standard deviation. The last three columns show the values for the transition between water-interface from the Wimley and White scale and the values from the UHS with its standard deviations (SD). Shaded regions are negative.
[a]The values from the literature have been inverted to match the direction of transfer from water to bilayer.

eral not as pronounced as in scales that were derived experimentally. This observation holds for the newly derived hydrophobicities: for example, although the GES scale ranges from −3.70 (Phe) to 12.30 (Arg), the Wimley and White scale from −2.09 (Trp) to 3.64 (Asp), the Hessa, White, and von Heijne ranges from −0.60 (Ile) to 3.49 (Asp), the values in the UHS derived here range only from −0.46 (Phe) to 0.90 (Lys). However, the correlation diagrams indicate that despite the deviation in absolute values the scales agree very well in general trends with correlation coefficients between $R = 0.804$ and $R = 0.956$. The UHS has higher correlation coefficients to knowledge-based scales such as PM1D and PM3D, and surprisingly, the highest correlation coefficient ($R = 0.956$) is found for the Hessa, White, and von Heijne scale, the most recent experimental scale considered (see below).

By disregarding structural context such as the level of exposure when deriving the scale the absolute size of the free energies derived is reduced. This originates in the MP database used for derivation containing only multispan MPs. These proteins have both hydrophobic cores and active polar sites within the trans-membrane region shielded from direct contact with the membrane lipids, as for example in ion channel proteins. Similarly, the

extra-membrane domains of these proteins also have both hydrophobic cores and polar active sites shielded from direct interaction with the solvent. As a result the absolute size of the free energies obtained is reduced. This has to be compared with, for example, an experimental scale that was observed for model peptides forming single α-helices within the membrane exposing their amino acid side chains almost completely to the lipid and having no extra-membrane domains with hydrophobic interior.

When compared with all other experimental scales, the "biological" transfer free energies from Hessa et al.[24] match the knowledge-based ones very closely in size and distribution. The scale yields the highest correlation coefficient of $R = 0.956$ to the UHS (compare Fig. 3 and Supp. Fig. 1). The reason for the smaller range is the measurements on an intact protein (E. coli leader peptidase) consisting of three TM segments where the structural context for the residue in question is maintained.

Hessa's study was extended to a position-dependent free energy scale derived from 324 (!) constructs.[23] The authors compared their hydrophobicity scale to a statistical distribution derived from known structures of helical MPs which showed the same trends as their experimentally derived potentials. We do not directly compare this

Table II
Chart Summarizing the Different Hydrophobicity Scales and Their Applicability

Scale	Ref.	year	Derivation[a]	α/β	Two-state/ three-state	Characteristics/applicability
Hopp and Woods	1	1981	Exp	n/a	2	Hydrophilicity scale for antigenic sites on the protein surface; derived from the values of Levitt[42]; some values were adjusted to fit immunochemical data of 12 proteins; for the proteins only the primary sequence was available; window size is six residues ≈ length of antigenic determinant
Goldman, Engelman, Steitz	2	1986	Exp	α	2	Hydrophobicity scale for single trans-membrane helices; semi-theoretical approach based on energetic considerations of residues undergoing hydrogen bonds in helices derived from experimental data in the literature; hydrophobicity scale as a sum of hydrophilic and hydrophobic components
Wimley and White	3,4	1996	Exp	α	2 + 3	Derived by measuring the partitioning energies of host-guest penta-peptides; whole residue scale that considers the polar peptide bond; interface: POPC vesicle interface; bilayer: n-octanol; for unfolded peptides in all three phases (solution, interface, bilayer)
Hessa et al.	23,24	2005/2007	Exp	α	2/pot	Designed trans-membrane helix within the Lep protein that is inserted via the Sec61 translocon; trans-membrane helix is 19-residue helix with amino acid in question incorporated in the center; measured fraction of singly vs. doubly glycosylated Lep molecules to derive the scale; therefore, applicable to folded MPs; scale has been extended to position-dependent free energy scale
Eisenberg and Weiss	43	1982	Cons	n/a	2	Normalized consensus scale derived from five different scales
Kyte and Doolittle	10	1982	Cons	n/a	2	Normalized consensus scale based on experimental observations of different scales; refinement by studying hydropathy plots of proteins of known X-ray structure
Guy	18	1985	Cons	n/a	2	Based on experimental and statistical results from several studies; considers solvent accessibility according to accessible layers of amino acids in globular proteins
Janin	7	1979	KB	n/a	2	Derived from X-ray structures of 22 soluble proteins; looked at molar fraction of buried and accessible residues
Punta and Maritan	8	2003	KB	α	2	Derived two membrane propensity scales from two trans-membrane helix databases using a simple perceptron algorithm; databases contained 118/228 trans-membrane helices; sequence identity of the proteins was 30%
Beuming and Weinstein	25	2004	KB	α	n/a	Calculated surface propensities of amino acids (probability of finding a residue on the surface of a trans-membrane protein); based on surface fractions of residues; considered 28 α-helical MPs
Senes et al.	9	2007	KB	α	2/pot	Calculated membrane depth-dependent potential for amino acid side-chains; considered 24 α-helical MPs
UHS		2008	KB	α/β	2 + 3	Derived from 60 known structures of folded MPs; considers folded structures both in solution and membrane bilayer; both α, β, and α/β structures were taken into account with approximately equal distribution of helices and strands; considers only depth in membrane bilayer and no accessibility or secondary structure
MHS		2008	KB	α	2 + 3	Derived from 16 known structures of folded MPs from mammalian organisms; only α-helical structures are taken into account; considers folded structures both in solution and membrane bilayer; considers only depth in membrane bilayer and no accessibility or secondary structure

[a]exp, experimental; cons, consensus; KB, knowledge-based; pot, potential.

scale to the three-state UHS because according to our definition of TM and TR thicknesses (see above), 19-residue α-helices would be too short to reach completely into solution and hence only TR and TM could have been compared with the UHS. Furthermore, to obtain single free energy values for each region from the Hessa study, the free energies would have to be averaged over a range, which removes information from the scale.
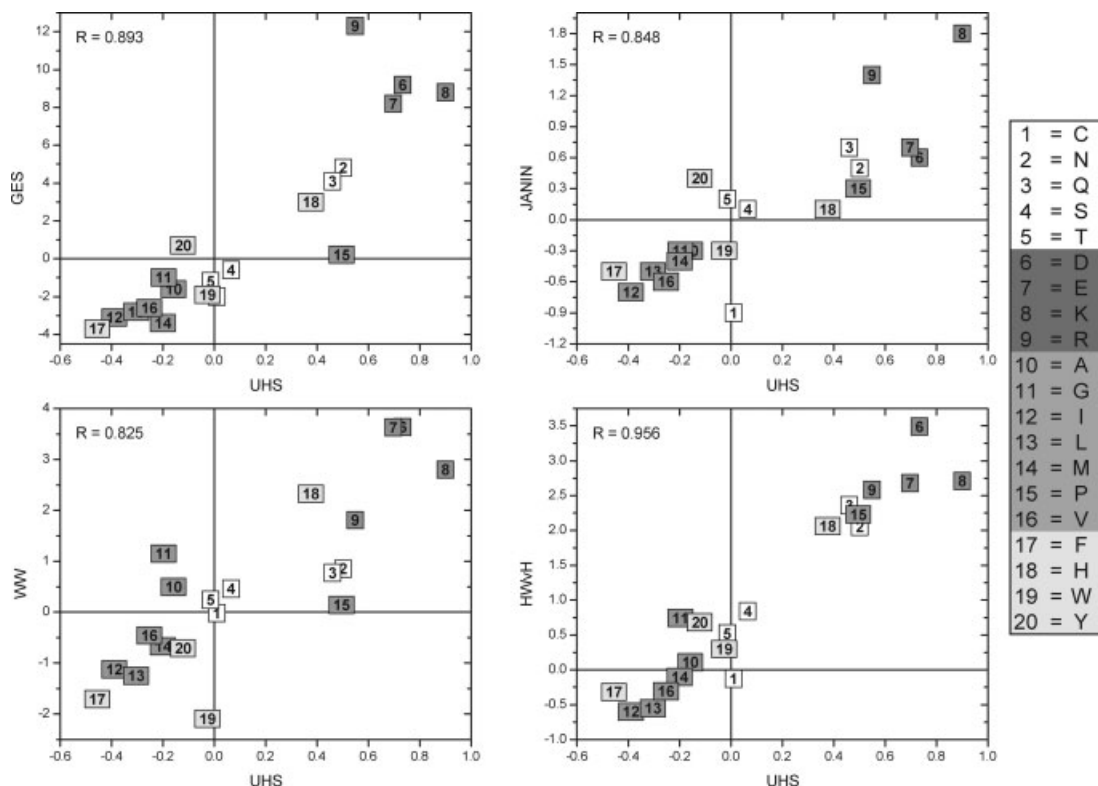
Figure 3

Plots showing the correlation between the UHS and the scales from GES, Janin, WW, and HWvH. The units are kcal/mol. The correlation coefficients are shown in the upper left corner of the plots. The amino acids are numbered according to the numbering scheme on the right and colored according to their class: white = polar, dark gray = charged, gray = apolar, light gray = aromatic. The highest correlation coefficient is seen for the scale of HWvH (Hessa, White and von Heijne) with a correlation coefficient of 0.956.

Table III

Free Energy Values of the UHS and MHS in kcal/mol

		UHS						MHS				
		TM ± SD		TR ± SD		SOL ± SD		TM ± SD		TR ± SD		SOL ± SD
Polar	C	−0.07	0.09	0.56	0.03	−0.22	0.06	−0.01	0.01	0.14	0.14	−0.09	0.10
	N	0.37	0.03	−0.14	0.01	−0.10	0.01	0.41	0.04	−0.15	0.03	−0.12	0.04
	Q	0.31	0.05	−0.01	0.03	−0.19	0.03	0.60	0.09	−0.13	0.07	−0.19	0.04
	S	0.02	0.03	0.02	0.03	−0.04	0.02	0.13	0.28	−0.01	0.07	−0.06	0.14
	T	−0.01	0.01	0.02	0.01	0.00	0.01	−0.02	0.01	−0.04	0.04	0.06	0.04
Charged	D	0.52	0.04	−0.08	0.03	−0.21	0.02	0.82	0.28	0.05	0.18	−0.34	0.05
	E	0.47	0.02	0.10	0.02	−0.31	0.01	0.84	0.05	0.06	0.10	−0.36	0.04
	K	0.69	0.03	−0.13	0.03	−0.22	0.03	0.99	0.15	−0.08	0.03	−0.30	0.04
	R	0.40	0.04	−0.11	0.02	−0.15	0.01	1.06	0.13	−0.22	0.08	−0.18	0.10
Apolar	A	−0.10	0.02	0.07	0.02	0.05	0.01	−0.15	0.01	0.12	0.02	0.07	0.01
	G	−0.09	0.02	−0.06	0.01	0.19	0.02	−0.07	0.03	0.05	0.03	0.03	0.06
	I	−0.22	0.02	0.12	0.02	0.18	0.02	−0.24	0.01	0.13	0.08	0.23	0.07
	L	−0.16	0.01	0.06	0.02	0.14	0.02	−0.26	0.03	0.15	0.07	0.24	0.00
	M	−0.12	0.03	0.01	0.05	0.13	0.04	−0.07	0.04	−0.06	0.02	0.16	0.02
	P	0.34	0.04	−0.08	0.02	−0.15	0.02	0.36	0.07	−0.09	0.07	−0.14	0.09
	V	−0.16	0.01	0.15	0.02	0.06	0.01	−0.22	0.03	0.22	0.05	0.09	0.01
Aromatic	F	−0.19	0.02	−0.02	0.02	0.34	0.01	−0.22	0.05	0.00	0.01	0.35	0.11
	H	0.29	0.03	−0.14	0.03	−0.07	0.04	0.55	0.41	−0.28	0.03	0.03	0.12
	W	0.08	0.02	−0.19	0.02	0.19	0.03	0.07	0.11	−0.24	0.15	0.36	0.24
	Y	−0.07	0.02	0.04	0.01	0.03	0.02	0.20	0.09	−0.13	0.04	−0.02	0.12

The table shows the knowledge-based values for the free energies in kcal/mol and their corresponding standard deviations (SD) for the 20 amino acids in the three regions of the membrane bilayer (TM), the transition region (TR), and the soluble region (SOL) for both scales, the UHS and the MHS. The shaded cells indicate the preference of the amino acid for that region. Note that Serine and Threonine in the UHS show almost no preference for any of the three regions.
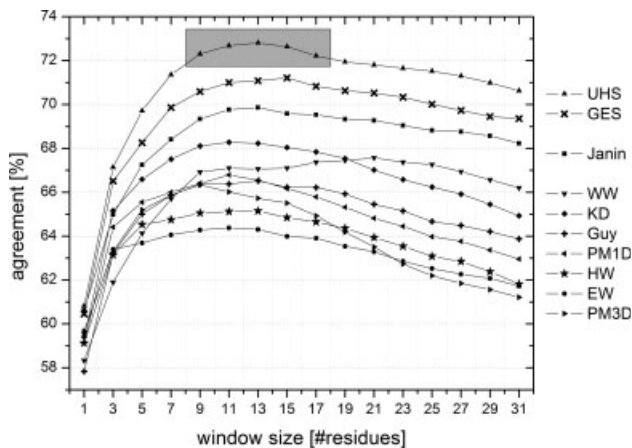
Figure 4

For predicting trans-membrane spans from the sequence, the hydrophobicity values are averaged over a number of residues ("window"). The percent per-amino acid agreements between prediction and known location of the residues were computed as a function of window size for the scales from the literature (EW: Eisenberg and Weiss,[17] GES: Goldman, Engelman, Steitz,[2] HW: Hopp and Woods,[1] KD: Kyte and Doolittle,[10] WW: Wimley and White,[5] Guy: Guy,[18] Janin: Janin,[7] PM1D and PM3D: Punta and Maritan[8]) and for the Unified Hydrophobicity Scale (UHS). The shaded region indicates a range of window lengths for the UHS, which all yield similarly good performance. The best performance is seen for the UHS and GES scales.

Triangular window function of 15 residues used for predicting trans-membrane spans

To test the usefulness of the derived UHS, it was applied towards predicting the state of an amino acid (TM, TR, or SOL) from primary sequence only. To achieve increased prediction accuracies, the hydrophobicities were averaged over a sequence window. This procedure allows for identification of spans of similar dielectric environments along the protein sequence.

Preliminary prediction trials have shown that the triangular window function performed better than the rectangular window. Because hydrophobicity is a local measure and therefore depends more on neighboring residues than on residues further away, this result is expected. In addition, these preliminary trials showed that the prediction accuracy in the two-state scenario (distinguishing TM from SOL region) is dependent on the window size as can be seen in Figure 4. Note, that there is a plateau range between 9 and 17 residues where all scales gave consistently good results. Therefore, for all further experiments we chose a window size of 15 residues. This number agrees with the average length of an α-helix spanning the core region of the membrane (15 residues × 1.5 Å rise = 22.5 Å membrane thickness).

Two-state scenario: UHS achieves 72.6% correct classifications

Table IV displays the percent agreement for TM and SOL. The scales of EW, HW, PM3D, PM1D, and Guy display a bias towards predicting an amino acid within the TM (>80% agreement) but poorly agree in the SOL (<50% agreement). Conversely, the scales of WW and

Table IV
Per Amino Acid Agreements for the Two-State Scenario

		PDB		
Pred		TM	SOL	avg
UHS				
	TM	70 ± 10	25 ± 7	
	SOL	30 ± 10	75 ± 7	
				73 ± 2
GES				
	TM	66	23	
	SOL	34	77	
				71
Janin				
	TM	72	32	
	SOL	28	67	
				70
KD				
	TM	76	39	
	SOL	24	61	
				68
WW				
	TM	48	13	
	SOL	52	87	
				67
HWvH				
	TM	11	1	
	SOL	89	99	
				55
Guy				
	TM	81	49	
	SOL	19	51	
				66
PM1D				
	TM	86	53	
	SOL	14	47	
				66
PM3D				
	TM	83	52	
	SOL	17	48	
				66
HW				
	TM	89	59	
	SOL	11	41	
				65
EW				
	TM	88	60	
	SOL	12	40	
				64

[a]The table shows the percentage per amino acid agreements for the two-state scenario between the prediction and the PDB for the hydrophobicity scales from the literature and the UHS. (TM) membrane bilayer; (SOL) soluble phase; (avg) average value of agreement between TM and SOL. The values are computed for a window size of 15 residues for averaging. The first four scales show similar performances for the TM and the SOL, whereas the other scales exhibit an uneven distribution.

HWvH bias towards the SOL (87% and 99%) with a lower performance in the TM (48% and 11%). These biases are indicative of offsets in the absolute TFE values when applied to intact multispan MPs and may not exist in other applications. This is not unexpected given that the reference point for every experimental scale is imposed by the experimental setup. For example, the bias in the WW scale originates from the fact that the scale was derived for unfolded peptides in both solution and membrane bilayer.

The other scales predict amino acids in an approximately balanced distribution (KD_{TM} = 76%, KD_{SOL} = 61%; $Janin_{TM}$ = 72%, $Janin_{SOL}$ = 67%; GES_{TM} = 66%, GES_{SOL} = 77%; UHS_{TM} = 70%, UHS_{SOL} = 75%). Although the good performance of our UHS scale is remarkable considering the simple approach it was derived with, it should be acknowledged that particularly good performance is expected in this experiment because the scale was derived with particular focus on such applications.

Even though the improvement of the UHS above the GES scale is small in the two-state scenario, this translates into a significant improvement when the accuracy of detecting full-length TM spans from the sequence is analyzed. Here the UHS identifies 81.1% of the TM spans, the GES scale identifies 76.6%, and the WW scale identifies 59.9% correctly.

False positive rate on soluble proteins is comparable to GES scale

To assess the over-prediction of regions in soluble proteins as being in the TM region, the scale was tested on a nonredundant set of soluble proteins (<25% sequence identity). This set was created by culling the PDB with the PISCES server with the same culling parameters as for the MHS and UHS (see Methods section). The database comprised 2,569 proteins with 3,538 chains and 526,422 amino acids.

Detailed results can be found in Supporting Table II. The scales of Hessa *et al.* and of Wimley and White predict amino acids as being in the SOL more than 95% of the time and hence have a corresponding false positive rate for predicting TM spans of smaller than 5%. This originates in the tendency of these scales to over-predict amino acids as being in the SOL. In result, both scales have a significantly reduced accuracy in the TM (compare Table IV). The scales of GES, Janin, KD, and the UHS have an approximately balanced distribution between SOL and TM and have a high agreement in SOL with a small number of false positives. Among these four scales, the UHS and GES perform comparably with an accuracy of ~86% in solution and ~14% over-prediction. Both scales are significantly better than the scales of Janin or KD in this experiment. The remaining scales (Punta and Maritan, Guy, Hopp and Woods, Eisenberg and Weiss) have a lower agreement in the SOL coupled with an increased rate of false positives caused by the tendency of these scales towards over-predicting amino acids as being in the TM.

The over-prediction of amino acids in soluble proteins as being in the TM region is reduced by about 10% when compared with the SOL of MPs (Supp. Tables II and IV). In MPs, many residues close to the membrane surface are within SOL in the two-state scenario. These residues are difficult to be accurately predicted as they often interact with the membrane surface and not only with the solvent. Further, the window for averaging will include some membrane amino acids for these residues. The absence of such difficult residues improves the prediction accuracy when looking at soluble proteins.

Comparison of UHS and GES for individual amino acids

Supporting Figures 3 and 4 summarize the results for individual amino acids for the two-state scenario in comparison to the GES scale, which gave for this experiment the best results besides the UHS. Both scales over-predict the polar amino acids Arg, Asn, Asp, Glu, Gln, and Lys in the SOL region. For the UHS, the average agreements are higher for the polar residues Arg, Asp, Glu, and Lys.

Comparing the GES scale with the UHS, the average agreements have increased most for Arg (51% to 58%), Cys (72% to 78%), and Glu (58% to 62%). Note that the average agreement in the UHS is lower than in the GES scale only for His (72% to 69%). This indicates a slightly better representation of polar residues in the present UHS.

Three-state scenario: UHS displays agreement of 57.1%

As discussed earlier, one strength of the UHS scale is that in contrast to many existing methods it distinguishes three regions. Only one of the nine scales used for comparison was derived with a TR region. Hence, comparison for the three-state scenario is limited to the Wimley and White (WW) scale. The data are summarized in Table V. For classifying an amino acid correctly in one of the three regions TM, TR, and SOL, the UHS scale achieves 57.1% as compared to 49.8% obtained for the WW scale. For the UHS, the prediction is balanced as indicated by the symmetry of the matrix (Table V). As already observed for the two-state scenario, the WW scale is biased in its prediction towards the SOL with an agreement of 89.1%. However, the agreement drops to 24.4% for the TR and 35.9% in the TM. Again, we wish to emphasize that these biases result from a different experimental setup and occur when applied to intact multispan MPs, and may not exist in other applications.

Table V
Per Amino Acid Agreements for the Three-State Scenario

Pred		PDB		
	TM	TR	SOL	Avg.
UHS				
TM	63 ± 11	29 ± 10	9 ± 6	
TR	23 ± 7	44 ± 3	26 ± 4	
SOL	13 ± 6	27 ± 9	64 ± 8	
				57 ± 3
WW				
TM	36	14	2	
TR	29	24	9	
SOL	35	62	89	
				50
MHS				
TM	71 ± 1	17 ± 4	5 ± 2	
TR	19 ± 3	48 ± 1	30 ± 4	
SOL	10 ± 2	35 ± 2	65 ± 2	
				61 ± 0

The table shows the percentage per amino acid agreements between the prediction and the PDB for the different regions for the UHS (with its standard deviation) in comparison to the Wimley and White scale. The performance of the MHS is also shown. The window size for averaging is 15 residues and (TM) represents the trans-membrane, (TR) the transition, and (SOL) the soluble region. The percentages were calculated by dividing the correctly predicted number of amino acids by the total number of amino acids in that region. An average agreement (Avg.) was calculated by averaging the percentages of agreement for the diagonal elements of the matrix. Although the average prediction agreement seems to be relatively low, note that there are three regions defined, so that the baseline probability is 33% and not 50% as in the two-state system. For the Wimley and White scale, both the octanol and the interface scale were used to establish a scale for three regions. The standard deviations for the UHS and MHS arise from cross-validation, whereas the scale of WW was tested on the whole dataset without cross-validation.

Supporting Figures 3 and 4 illustrate the individual amino acid agreements for the three-state scenario in comparison to the Wimley and White scale. As in the two-state scenario, the polar residues Arg, Asn, Asp, Glu, Gln, His, Lys, and Ser are predicted in a more balanced manner in the UHS than in the WW scale. When comparing the overall prediction accuracies, all amino acids either display an improvement or at least a similar accuracy for the UHS. Highest changes are observed for Asp and Glu (from 36% to 47%), Asn (from 41% to 50%), and His (from 44% to 53%).

It should be noted that the Wimley and White scale was derived for unfolded peptides in all three phases (solution, interface, and membrane bilayer). In contrast to folded secondary structure elements or domains where most backbone amide and carbonyl groups are undergoing hydrogen bonds, unfolded peptides can only engage in hydrogen bonds with polar solvents such as water, not with hydrophobic solvents or the membrane core. This fact offsets the WW scale towards a preference of the SOL region which explains the over-prediction for that region. Obviously, the Wimley and White scale was not derived for the current application of predicting TM spans from the sequence only,[3–5,44] and is an exceptional scale in its own right. We focus on its performance because it is the only available scale for the three-state

scenario we can use for comparison. The lack of suitable scales for the present application presents another justification for the development of the UHS.

The UHS enables prediction of TM spans from sequence only

We realize that different and more specialized hydrophobicity scales can be derived if assumptions on secondary structure (like separation of α-helices from β-strands) or tertiary structure (like level of exposure) were made. On purpose, such assumptions were forgone to make the hydrophobicity scale applicable in the absence of any structural information about the sequence of interest.

We also abstained from use of secondary structure prediction techniques because their accuracy is limited and most of these tools are highly specialized. However, we appreciate that the incorporation of secondary structure and/or the exposure of an amino acid is likely to be superior to the presented scale for certain applications.

The UHS is largely independent of the protein fold

To date, only a small fraction of the proteins stored in the PDB are MPs and only about 60 MP folds are known. When deriving a knowledge-based scale from such a limited database, the question arises whether this scale is applicable to the MP universe whose folds have not been elucidated yet. The scale could, for example, have a compositional bias of certain amino acid types due to the under-representation of distinct folds in the database.

Although we believe that such a bias is unavoidable given the very limited number of MP structures known, we argue that it is small as the hydrophobicity scale is governed by more general rules of MP fold formations such as α-helix/α-helix packing or β-barrel formation. We tested this hypothesis by excluding folds one by one when deriving the UHS scale and analyzing the effects on the hydrophobicity values. Note that for some MP folds multiple representatives are found in the database of 60 proteins, as it was culled purely by sequence and not by fold identity. Further we tested the prediction accuracies of these "leave-one-fold-out" UHS scales on the excluded folds. The details of this experiment are included in the supporting information data section. Briefly, we find the hydrophobicity values robust with respect to exclusion of a single fold (changes in hydrophobicity values are on average well below one standard deviation) and the prediction accuracy for TM and SOL regions is within 2.4% to the one observed with the UHS scale.

Applications of the scale

The UHS is optimized for usage as reference hydrophobicity values in computational protein structure prediction of α-helical and β-strand multispan MPs. The scale fills a gap because most existing scales were optimized only for the usage with α-helical MPs and distinguish only the two-states (TM and SOL). Furthermore, it can be used for the prediction of trans-membrane spans from genomic data (see below), in the early stages of a MP structure determination project when no structural information is available, or to assess the overall and local stability of folded multispan MPs. To exemplify the latter, the UHS values for Trp, Tyr, and Phe were compared with Lukas Tamm's thermodynamic free energy changes (see Table I in Ref. 45) by measuring the unfolding of wt OmpA and OmpA mutants as described in Ref. 45. The correlation coefficients are 0.715 for the single mutants, and 0.759 for the double mutants, excluding one outlier Y168A. No extensive conclusions can be drawn from the moderate agreement with these 11 data points for three amino acids, however, we believe that this possible application of the UHS warrants further investigation.

A hydrophobicity scale for mammalian α-helical membrane proteins

Because the amino acid occurrences are variable among organisms and there is interest in applying hydrophobicity scales to ORFs of mammalian genomes (specifically the human genome), a hydrophobicity scale was derived only from mammalian proteins. A database of 16 mammalian MPs was created as described in the Methods section and a mammalian scale (MHS) was derived using two-fold cross-validation. The MHS was established for the two- and three-state scenario. The scale will be most applicable to α-helical proteins because the database used for the derivation contained exclusively multispan α-helical MPs. The hydrophobicity values and their standard deviations are given in Tables I and III. The standard deviations are somewhat larger for the MHS when compared with the UHS because of the smaller dataset and the only two-fold cross-validation.

Overall amino acid abundance is quite similar between bacterial and mammalian MPs (data not shown) with an average difference of 0.18 when the amino acid abundances for all amino acids are normalized to 20. Ala, Asn, and Gly are somewhat more abundant in the bacterial dataset with differences of 0.32, 0.25, and 0.60, respectively, whereas Leu and Pro are more abundant in the mammalian dataset (−0.32 and −0.26). Furthermore, comparing the distribution between TM and SOL, it was found that Arg, Gly, Phe, and Tyr tend to be more abundant in the TM in the bacterial dataset than in the mammalian dataset. The differences for these amino acids are 0.29, 0.29, 0.26, and 0.50 when the occurrence for each amino acid is normalized to 2.
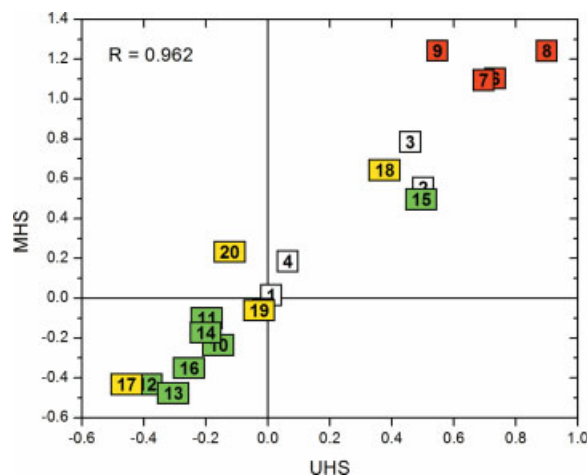

Figure 5

Correlation plot for the hydrophobicity values in kcal/mol between the Unified Hydrophobicity Scale and the Mammalian Hydrophobicity Scale with the amino acids being numbered according to the scheme in Figure 3. white = polar, red = charged, green = apolar, yellow = aromatic. [Color figure can be viewed in the online issue, which is available at www.interscience.wiley.com.]

Overall UHS and MHS are similar with deviations of 1.3 standard deviations on average and 3.8 standard deviations at maximum for Glu. Even though these seem to be relatively large changes, the change in actual numbers remains small, because of the small standard deviations for the UHS. A correlation plot of the two scales is shown in Figure 5 with a correlation coefficient of 0.962.

Comparison of the hydrophobicity values from the UHS with the MHS reveals that the largest deviations occur for Arg (UHS: 0.55 kcal/mol/MHS: 1.24 kcal/mol), Asp (0.73/1.10), Glu (0.70/1.09), Leu (−0.30/−0.48), Lys (0.90/1.24), and Tyr (−0.12/0.23). A test of the prediction accuracy of the MHS is available in Table V and in Supporting Table V. Briefly, the scale achieves an average prediction accuracy of 83.1% in the two-state scenario and 61% in the three-state scenario (see Table V).

It is important to note that although this is the first mammalian hydrophobicity scale ever derived, care has to be taken in its application. The dataset used for its derivation is with only 16 MPs very small and does not guarantee very accurate hydrophobicity values. A refinement of the scale is to be expected when more MPs structures are elucidated. Nevertheless, we hope the MHS will find widespread application in the scientific community.

Four examples show that the UHS accurately reflects the character of α-helical and β-barrel MPs

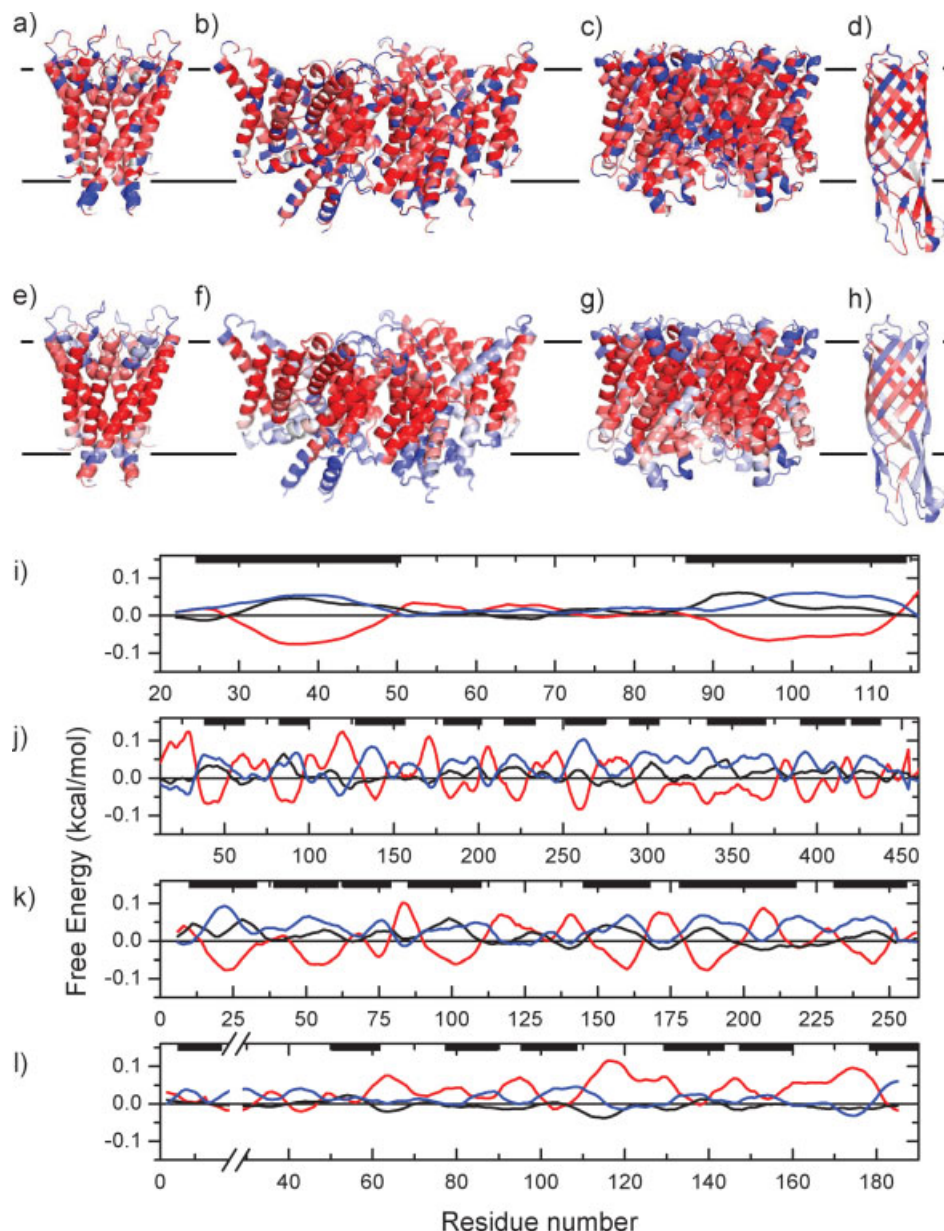Four proteins not present in the MP database (used for derivation of the UHS) were used as examples to

Figure 6

The derived UHS has been used to calculate the free energies (with a window length of 15 residues) for four examples: (**a, e, i**) KcsA, potassium channel (PDB code 1K4C); (**b, f, j**) ClC, chloride channel (PDB code 1KPK); (**c, g, k**) GlfP, Glycerol facilitator protein (PDB code 1LDI); and (**d, h, l**) OmpW, outer membrane protein W (PDB code 2F1T). The upper panels (a–d) show the three-state predictions from the sequence without any averaging procedure mapped onto the known crystal structure. The central panels (e–h) display the predictions for a window length of 15 residues. Dark blue indicates a prediction for the aqueous phase, white indicates interface, and dark red indicates a prediction for the TM. Lighter colors refer to a lower confidence in the prediction (as seen by smaller differences between the lowest and second lowest free energy in the bottom panels of the figure). The location of the membrane is displayed by the black lines. The lower panels (i–l) show the predictions of the free energies vs. the residue number as in panels (e–h) (red is TM, black is TR, and blue is SOL). Membrane locations are indicated by the black bars at the top. Panel (i) shows one of four identical chains, (j) shows one of two chains (chain A), (k) shows one of four identical chains, and (l) shows the whole protein sequence.

demonstrate the usefulness of the UHS and the prediction algorithm. The hydrophobicity values of the UHS for all residues in the sequence were mapped onto the known crystal structures in Figure 6(a–d). In Figure 6(e–h), the average free energy values were mapped onto the same crystal structures to illustrate the prediction of TM, TR, and SOL regions. Panels (i–l) in Figure 6 show the predicted free energies averaged over a window length of 15 residues (compare to panels (e–h)) vs. the residue number.
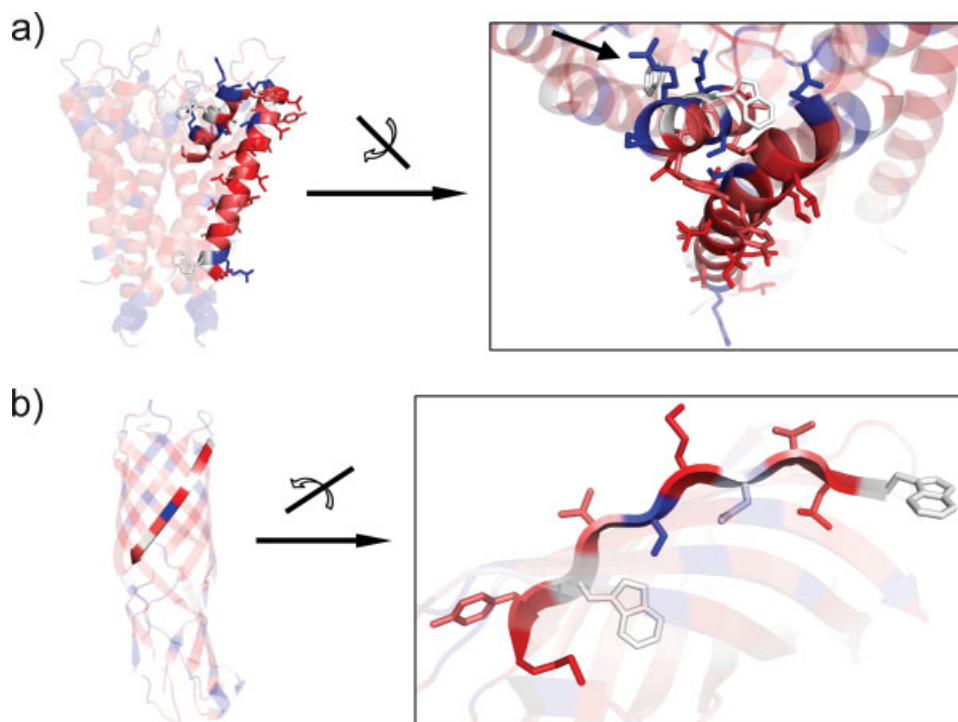
Figure 7

Close-ups of Figure 6 (a, d). The figure demonstates the ability of the UHS to correctly identify the structural context of the amino acids within a functional protein. Figure 7(**a**) displays the prediction for the pore helix of the KcsA potassium channel (short helix on the top). Figure 7(**b**) demonstrates that the UHS is clearly able to distinguish the different hydrophobicities of the side-chains in the β-barrel. More details are given in the Results and Discussion section.

UHS distinguishes core TM α-helices from functional sites in potassium channel KscA

The first example [Fig. 6(a,e,i)] is the crystal structure of the potassium channel KscA which was determined by Roderick McKinnon *et al.* at a resolution of 2.0 Å (PDB code 1K4C). This example demonstrates the ability of the UHS to distinguish a typical hydrophobic, membrane-spanning α-helix from a functional site such as the pore α-helix and the selectivity filter. The pore α-helix is too short to even reach the center of the bilayer and the attached loop region returns to the extra-cellular side. This region is rich in polar amino acids as it is exposed to the SOL and has no direct contact to the membrane. The UHS clearly identifies the pore α-helix as an amphiphilic helix [short helix on the top of Fig. 7(a)] where the polar side-chains point to the aqueous cavity (arrow) and the apolar side-chains are in contact with other hydrophobic α-helices. This compares to a fully hydrophobic α-helix (long helix at the bottom) where all nonpolar side-chains interact with the hydrophobic environment. It illustrates that the UHS is well able to identify the structural context of the individual residues even though no structural information is used in its derivation.

The prediction algorithm is clearly able to distinguish the membrane region from the sequence only. Figure 6(i) demonstrates that the TMs are perfectly identified with a very high confidence and with their approximate lengths. However, the pore helix and selectivity filter of the protein have a small preference for the SOL region, which is indicated by the light blue α-helices at the top of the molecule (6e). This is not surprising because—as detailed above—both the structural features are not in contact with the membrane at all but form a polar pore filled with water and ions [see Fig. 7(a)].

Chloride channel ClC

The second example [Fig. 6(b,f,j)] is the crystal structure of the chloride channel ClC determined by Roderick McKinnon and coworkers at a resolution of 3.5 Å (PDB code 1KPK). In this case, all TM α-helices are reliably identified and the predicted membrane locations agree well with the actual ones. However, the lengths deviate from the predicted spans slightly more than in the first example.

Glycerol facilitator protein GlfP

The third example [Figure 6(c,g,k)] is the crystal structure of the glycerol facilitator protein GlfP determined by

Robert Stroud *et al.* at a resolution of 2.7 Å (PDB code 1LDI).

Generally, the UHS is able to identify polar residues within the trans-membrane domains of the protein which mostly face the interior of the protein and are therefore protected from the hydrophobic environment of the membrane bilayer. The α-helix at residues 204–217 is a short helix dipping into the membrane and the attached loop residues return to the same side of the membrane. The UHS clearly identifies this short α-helix as an amphiphilic helix where the polar side of this short helix faces inwards into one of the four channels of the homo-tetramer. Again, this shows the capability of the UHS to distinguish between regular, fully hydrophobic trans-membrane α-helices and functional sites in the protein.

Figure 6(k) shows that the trans-membrane α-helices are correctly identified with a high reliability. The lengths of the α-helices agree well with the actual lengths except for the one α-helix at residue numbers 175–215 which is predicted to be too short. As discussed, under-prediction is unsurprising due to the amphiphilicity of this short α-helix that faces one of the pores of the channel. In Figure 6(g), this α-helix is the light blue helix on the lower left side of the protein.

The UHS identifies alternative hydrophobicity pattern in the β-barrel of the outer membrane protein W

The fourth example (Fig. 6(d,h,l)) is a β-barrel protein which is the crystal structure of the outer membrane protein W (OmpW) determined by van den Berg and Tamm *et al.* at a resolution of 3.0 Å (PDB code 2F1T). Figure 7(b) shows that the UHS correctly identifies the polarity of the side-chains pointing to the aqueous interior of the β-barrel, whereas apolar side-chains face the hydrophobic milieu of the membrane bilayer. It can be seen, that consecutive side-chains along the β-strand alternately face the polar interior and apolar membrane environment. These patterns are nicely detected by the UHS [Fig. 6(d)]. This demonstrates the efficiency of the UHS to depict structural features of the amino acids although no structural information is required for the application of the UHS.

Figure 6(h,l) show that for β-barrels the prediction has lower confidence and only some of the trans-membrane spans are identified. However, this behavior is expected because this simple window function is insufficient to reliably identify trans-membrane spans if an alternating pattern of hydrophobicity values complicates the prediction, as is the case for β-barrel proteins. To optimize the prediction accuracies for β-barrels, we plan to utilize the UHS as an input for an artificial neural network or a hidden Markov model in the future.

In summary, these four examples illustrate the ability of the UHS scale to accurately reflect the hydrophobicity

of a certain residue within a folded protein. In particular, the scale distinguishes nicely between the core of the protein and functional sites and highlights the alternating hydrophobicity pattern seen in β-barrel proteins. The scale is therefore suitable as input for MP secondary and tertiary structure prediction tools. This was demonstrated by the usage of the UHS for prediction of trans-membrane spans from sequence only. Although the prediction accuracies are somewhat lower for β-barrel proteins when using such a simple averaging scheme, they are better than random (60% average prediction accuracy in the two-state scenario and 45% in the three-state scenario). For α-helical bundles, the prediction accuracy increases up to 77% in the two-state scenario and even 66% in the three-state scenario (compared with 33% for a random prediction).

CONCLUSIONS

In this article, we derive a three-state UHS exclusively from multispan MPs of known structure. The database of MPs contained both α-helical and β-barrel proteins. The absolute hydrophobicity values in the UHS range between −0.46 kcal/mol for Phe and 0.90 kcal/mol for Lys. This reduced amplitude when compared with most experimentally derived scales was previously observed for other knowledge-based scales and results from averaging over a wide variety of structural contexts, in particular different degrees of burial in the protein core or different types of secondary structure. This makes the UHS applicable for the prediction of trans-membrane spans from the proteins primary sequence only.

This scale is applicable as an unbiased average hydrophobicity value for an amino acid that is equally valid for both α-helical and β-strand multispan MPs, which is of high importance for computational protein structure prediction. Furthermore, it can be used in the early stages of a membrane protein structure determination project when no structural information is available. The overall and local stability of folded multispan MPs can be assessed as demonstrated for OmpA. It can also be used for the prediction of trans-membrane spans from genomic data. For this application, we specifically derived a hydrophobicity scale only from mammalian proteins (MHS) to be applicable to mammalian genomes or the human genome in particular. This scale is optimized for α-helical multispan MPs and reaches average accuracies of up to 83%.

In general, we observe a bias in many existing hydrophobicity scales when applied to folded, multispan MPs. This offset applies to both the reference point of the scale (which we chose to be multispan MPs) as well as the absolute size of the free energy values. These biases are imposed by the respective experimental setup and may not exist in other applications. It emphasizes the impor-

tance to carefully choose the hydrophobicity scale based on the given task.

The UHS scale was tested for predicting trans-membrane spans from the primary sequence only. It was found that the prediction improves when free energies are averaged over a window of 9–17 amino acids with a triangular weight giving the central amino acid the highest influence. For a two-state prediction scenario (classifying an amino acid as being either in the TM or SOL), it was found that in comparison to other hydrophobicity scales the UHS yields an average prediction accuracy of 73%. The scales of GES (71%) and Janin (70%) perform almost as well. For a three-state scenario that includes a TR region, the UHS performs at an accuracy of 57%. This is significantly better than the WW scale (50% correct classifications).

Application of the UHS scale to four proteins illustrates its ability to very accurately map the hydrophobicity of a certain residue within a folded protein. In particular, the scale distinguishes nicely between the core of the protein and functional sites and highlights the alternating hydrophobicity pattern seen in β-barrel proteins. The scale is therefore suitable as input for membrane protein secondary and tertiary structure prediction tools. This was demonstrated by the usage of the UHS for the prediction of trans-membrane spans from the sequence only.

When predicting trans-membrane spans in these four proteins, the lengths and positions of the predicted α-helices agree well with the actual lengths and locations. For β-barrel proteins, the prediction tool is less reliable because the alternating hydrophobicity pattern thwarts the effectiveness of the simple averaging procedure. This is a general observation for β-barrel proteins across the scales and does not imply that the UHS poorly describes the characteristics of β-barrel proteins. It rather emphasizes the fact that the type of window function is not optimal for the prediction of β-barrels.

ACKNOWLEDGMENTS

REFERENCES

1. Hopp TP, Woods KR. Prediction of protein antigenic determinants from amino acid sequences. Proc Natl Acad Sci USA 1981;78:3824–3828.
2. Engelman DM, Steitz TA, Goldman A. Identifying nonpolar trans-bilayer helices in amino acid sequences of membrane proteins. Annu Rev Biophys Biophys Chem 1986;15:321–353.
3. Wimley WC, White SH. Experimentally determined hydrophobicity scale for proteins at membrane interfaces. Nat Struct Biol 1996;3:842–848.
4. Wimley WC, Creamer TP, White SH. Solvation energies of amino acid side chains and backbone in a family of host-guest pentapeptides. Biochemistry 1996;35:5109–5124.
5. White SH, Wimley WC. Membrane protein folding and stability: physical principles. Annu Rev Biophys Biomol Struct 1999;28:319–365.
6. Jayasinghe S, Hristova K, White SH. Energetics, stability, and prediction of transmembrane helices. J Mol Biol 2001;312:927–934.
7. Janin J. Surface and inside volumes in globular proteins. Nature 1979;277:491–492.
8. Punta M, Maritan A. A knowledge-based scale for amino acid membrane propensity. Proteins 2003;50:114–121.
9. Senes A, Chadi DC, Law PB, Walters RF, Nanda V, Degrado WF. E(z), a depth-dependent potential for assessing the energies of insertion of amino acid side-chains into membranes: derivation and applications to determining the orientation of transmembrane and interfacial helices. J Mol Biol 2007;366:436–448.
10. Kyte J, Doolittle RF. A simple method for displaying the hydropathic character of a protein. J Mol Biol 1982;157:105–132.
11. Chothia C. The nature of the accessible and buried surfaces in proteins. J Mol Biol 1976;105:1–12.
12. Nozaki Y, Tanford C. The solubility of amino acids and two glycine peptides in aqueous ethanol and dioxane solutions. Establishment of a hydrophobicity scale. J Biol Chem 1971;246:2211–2217.
13. Hine J, Mookerjee PK. Intrinsic hydrophilic character of organic compounds—correlations in terms of structural contributions. J Org Chem 1975;40:292–298.
14. Wolfenden RV, Cullis PM, Southgate CCF. Water, protein folding, and the genetic-code. Science 1979;206:575–577.
15. Rose GD. Prediction of chain turns in globular proteins on a hydrophobic basis. Nature 1978;272:586–590.
16. Rose GD, Roy S. Hydrophobic basis of packing in globular proteins. Proc Natl Acad Sci USA 1980;77:4643–4647.
17. Eisenberg D, Weiss RM, Terwilliger TC. The hydrophobic moment detects periodicity in protein hydrophobicity. Proc Natl Acad Sci USA 1984;81:140–144.
18. Guy HR. Amino acid side-chain partition energies and distribution of residues in soluble proteins. Biophys J 1985;47:61–70.
19. Fauchere JL, Do KQ, Jow PY, Hansch C. Unusually strong lipophilicity of 'fat' or 'super' amino-acids, including a new reference value for glycine. Experientia 1980;36:1203–1204.
20. Wolfenden R, Andersson L, Cullis PM, Southgate CC. Affinities of amino acid side chains for solvent water. Biochemistry 1981;20:849–855.
21. Wertz DH, Scheraga HA. Influence of water on protein structure. An analysis of the preferences of amino acid residues for the inside or outside and for specific conformations in a protein molecule. Macromolecules 1978;11:9–15.
22. Robson B, Osguthorpe DJ. Refined models for computer simulation of protein folding. Applications to the study of conserved secondary structure and flexible hinge points during the folding of pancreatic trypsin inhibitor. J Mol Biol 1979;132:19–51.
23. Hessa T, Meindl-Beinker NM, Bernsel A, Kim H, Sato Y, Lerch-Bader M, Nilsson I, White SH, von Heijne G. Molecular code for transmembrane-helix recognition by the Sec61 translocon. Nature 2007;450:U1026–U1032.
24. Hessa T, Kim H, Bihlmaier K, Lundin C, Boekel J, Andersson H, Nilsson I, White SH, von Heijne G. Recognition of transmembrane helices by the endoplasmic reticulum translocon. Nature 2005;433:377–381.
25. Beuming T, Weinstein H. A knowledge-based scale for the analysis and prediction of buried and exposed faces of transmembrane domain proteins. Bioinformatics 2004;20:1822–1835.
26. Available at: http://icb.med.cornell.edu/crt/ProperTM/.
27. Yarov-Yarovoy V, Schonbrun J, Baker D. Multipass membrane protein structure prediction using Rosetta. Proteins 2006;62:1010–1025.

28. Yarov-Yarovoy V, Baker D, Catterall WA. Voltage sensor conformations in the open and closed states in ROSETTA structural models of K(+) channels. Proc Natl Acad Sci USA 2006;103:7292–7297.

29. Barth P, Schonbrun J, Baker D. Toward high-resolution prediction and design of transmembrane helical protein structures. Proc Natl Acad Sci USA 2007;104:15682–15687.

30. Sippl MJ. Knowledge-based potentials for proteins. Curr Opin Struct Biol 1995;5:229–235.

31. Poole AM, Ranganathan R. Knowledge-based potentials in protein design. Curr Opin Struct Biol 2006;16:508–513.

32. Tusnady GE, Dosztanyi Z, Simon I. PDB_TM: selection and membrane localization of transmembrane proteins in the protein data bank. Nucleic Acids Res 2005;33(Database issue):D275–D278.

33. Tusnady GE, Dosztanyi Z, Simon I. TMDET: web server for detecting transmembrane regions of proteins by using their 3D coordinates. Bioinformatics 2005;21:1276–1277.

34. Tusnady GE, Dosztanyi Z, Simon I. Transmembrane proteins in the Protein Data Bank: identification and classification. Bioinformatics 2004;20:2964–2972.

35. Wang GL, Dunbrack RL. PISCES: recent improvements to a PDB sequence culling server. Nucleic Acids Research 2005;33:W94–W98.

36. Wang GL, Dunbrack RL. PISCES: a protein sequence culling server. Bioinformatics 2003;19:1589–1591.

37. Wiener MC, White SH. Structure of a fluid dioleoylphosphatidylcholine bilayer determined by joint refinement of X-ray and neutron diffraction data. III. Complete structure. Biophys J 1992;61:434–447.

38. Shortle D. Composites of local structure propensities: evidence for local encoding of long-range structure. Protein Sci 2002;11:18–26.

39. Yau WM, Wimley WC, Gawrisch K, White SH. The preference of tryptophan for membrane interfaces. Biochemistry 1998;37:14713–14718.

40. Ulmschneider MB, Sansom MS, Di Nola A. Properties of integral membrane protein structures: derivation of an implicit membrane potential. Proteins 2005;59:252–265.

41. White SH, von Heijne G. Transmembrane helices before, during, and after insertion. Curr Opin Struct Biol 2005;15:378–386.

42. Levitt M. A simplified representation of protein conformations for rapid simulation of protein folding. J Mol Biol 1976;104:59–107.

43. Eisenberg D, Weiss RM, Terwilliger TC, Wilcox W. Hydrophobic Moments and Protein-Structure. Faraday Symposia of the Chemical Society 1982;17:109–120.

44. White SH, Wimley WC. Hydrophobic interactions of peptides with membrane interfaces. Biochim Biophys Acta 1998;1376:339–352.

45. Hong H, Park S, Jimenez RH, Rinehart D, Tamm LK. Role of aromatic side chains in the folding and thermodynamic stability of integral membrane proteins. J Am Chem Soc 2007;129:8320–8327.